Synoptic Radio Observations

E. J. Schmahl and M. R. Kundu

University of Maryland, College Park, MD, 20742, USA

Abstract. The microwave flux of the Sun is responsive to the same conditions that produce magnetically structured radiation at visible and X-ray wavelengths, and so the solar flux at high radio frequencies (e.g. 2800 MHz, or 10.7 cm) has, since the 1940's, been used as a proxy for solar optical variations. More recently, but still dating from the 1950's, the Toyokawa/Nobeyama measurements of flux at 1000, 2000, 3750, and 9400 MHz have supplemented the 2800 MHz time series. These synoptic measurements at lower and higher frequencies greatly add to the spectral information that is available on timescales ranging from days to decades.

We present a brief, but abridged, history of long-time-scale synoptic radio observations, with several of the more interesting results of recent years. In particular, we point out the significance of the observed spectral variations that parallel the brightness variations, and summarize the new concept of the "rotationally-modulated microwave component". Finally, we show that the calibration of the ground-based radio measurements has proven to be so stable that it may be possible to "bridge" short gaps in measurements of total solar irradiance, should that become necessary due to launch failures or satellite malfunctions.

1. Introduction

Synoptic radio observations of the Sun started in Canada in November, 1946, when Covington used a 4-ft reflector from a Type IIIC Gun Laying radar system to start recording the solar flux at 3-cm wavelength.

1.1. A Brief History

In 1947, Covington's landmark measurements developed into a regular observing program at 10.7 cm (Covington 1988). The daily flux was measured in Ottawa at Algonquin Radio Observatory until June 1991, when the program was moved to Penticton at Dominion Astrophysical Observatory, three time zones west, where it continues today (Tapping 1997; http://www.drao.nrc.ca/icarus/www/sol_home.shtml). Fig. 1 shows the daily flux for the period February 1947 to September 1997.

Within a year, synoptic measurements began at Sydney, but these were not continuous after the 1950's. In late 1951, regular observations began in Japan at 3750 MHz (8.0 cm), and in 1956 these were supplemented by observations at 1000, 2000, and 9400 MHz (30, 15 and 3.2 cm, respectively). These data
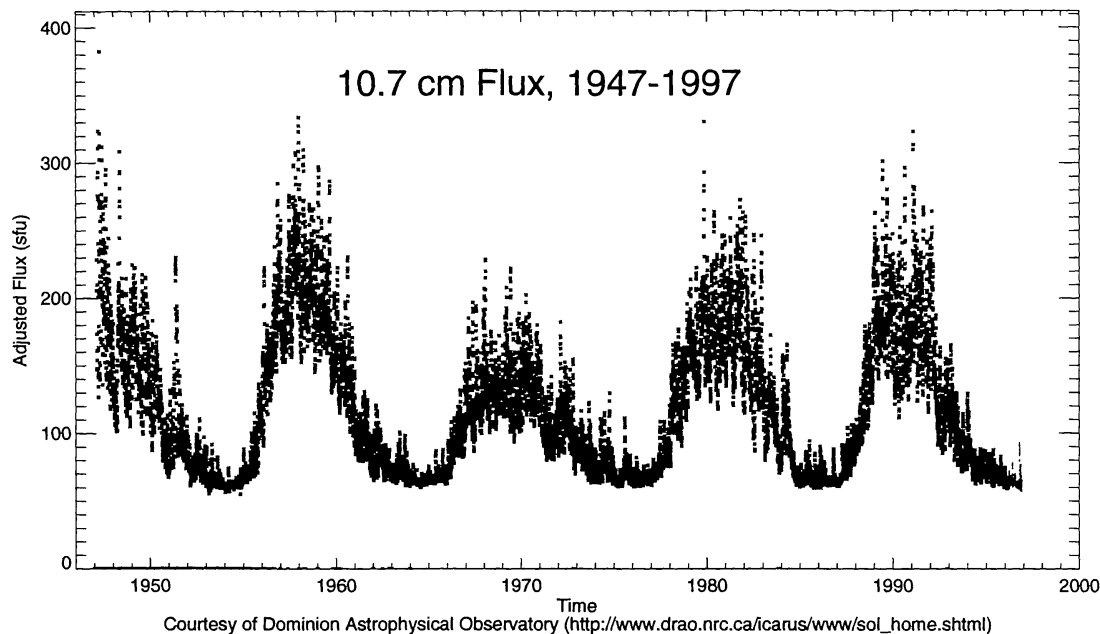
Figure 1.   The daily flux for the period February 1947 to September 1997. (Courtesy of K. Tapping, Dominion Astrophysical Observatory)

were obtained continuously to the present day. By 1958, several other observatories had started synoptic programs, and these multiplied many-fold during the 1960's.

The Sagamore Hill Solar Radio Observatory began operating solar patrols at 8800, 4995, 2695, 1415, and 609 MHz in 1966. The patrol was extended to 15400 MHz in 1967, to 242 MHz in early 1969, and to 410 MHz in early 1971.

In the mid 1960's it became evident that there were serious discrepancies in the relative flux measurements made at different observatories, and an URSI commission was assembled to achieve a uniform calibration. The working group, led by H. Tanaka, agreed that the pyramidal horn coupled with careful zenith and background measurements provided an accurate and stable calibration (Tanaka et al. 1973). The Toyokawa patrol had adopted this technique as early as 1965, and the earlier measurements were corrected for errors of order 5%. Subsequently, most observatories had relative disagreements of less than ±1%, and the long-term stability of the Toyokawa fluxes is much better than that. Fig. 2 shows a time series for the 1980-1989 period using 1000-9400 MHz data from Toyokawa and 2800-MHz (10.7 cm) data from Ottawa.

1.2. Proxy measurements

The 10.7-cm flux has been used as a proxy for many solar features and properties. Among these are:

Sunspot Number: Using 40 years of measurements, Tapping obtained the following relationship between the 10.7-cm flux and sunspot number: SN = $1.147 \times F_{10.7} - 73.21$

Sunspot Area: Denisse (1948) found a 76% correlation between the 10.7-cm flux and the area of sunspots.
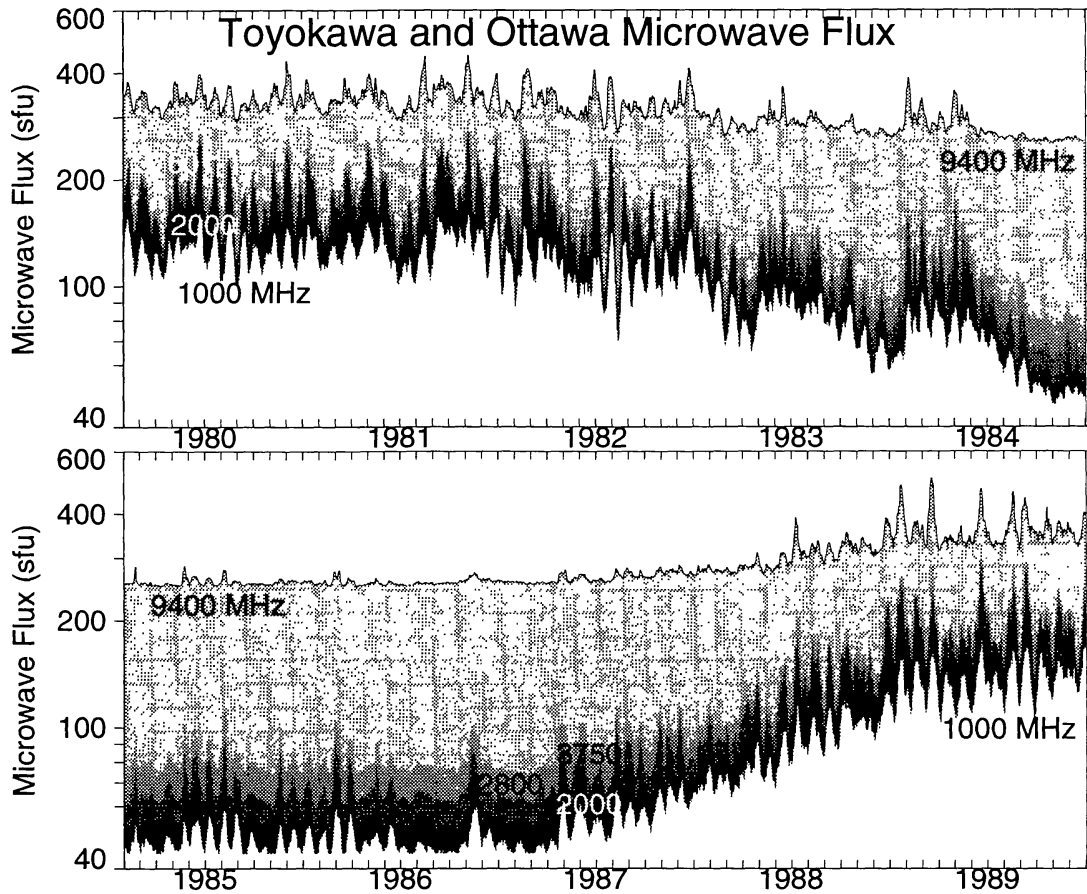
Figure 2.   Fluxes for the 1980-1989 period using 1000-9400 MHz data from Toyokawa and 2800-MHz (10.7 cm) data from Ottawa.

E-layer Ionization: Denisse & Kundu (1957), Kundu & Denisse (1958) found a good correlation between earth's E-layer ionization index and the 10.7 cm flux, and concluded that the source of solar X-rays responsible for this layer of the ionosphere lay below the height of the source of ∼ 50-cm radio emission.

Lyman β**:** Hinteregger et al. (1981) made early use of the 10.7-cm flux as a proxy for the AE-1 measurements of the Lyman lines. Later, Bouwer (1992) found that when the long-term variations and the short-term variations of the 2800-MHz flux were used separately, a better proxy resulted.

Mg II: Donnelly et al. (1992) used regression fits to the 10.7-cm flux to mimic the behavior of the chromospheric UV line Mg II. Mid-term (81-day) variance was matched at the r=0.99 level, but short-term variations required the addition of the Photometric Sunspot Index (PSI) for good results.

EUV Fluxes: Neupert (1992) found that simple regression with the 10.7-cm flux produced mixed results. Independently, Tobiska (1992) used the smoothed and daily 10.7-cm fluxes in conjunction with optical data to provide a proxy for several EUV bands. This led to the SERF3 model adopted by the Solar Electromagnetic Radiation Study for Solar Cycle 22.

Total Irradiance: Schmahl & Kundu (1995) used the 10.7-cm flux along with 4 other frequencies to obtain a useful proxy for the short and intermediate-term variations of the total irradiance.

2.   Rotational Modulation

One of the recurring themes in the attempts to use the 10.7 cm flux for a proxy is that the emission is produced partially by coronal and partially by chromospheric plasmas. The usual ploy for separating these components is to use a "smoothed" 81-day (or so) time series along with a daily time series, and apply regression methods with each considered as an independent time series. Multi-frequency measurements also would have been useful for this purpose (as we will show) but these have been employed only rarely (e.g. Pap & Tlamicha 1992; Schmahl & Kundu 1994, 1995).

A problem with creating two time series from one by convolving with a low-pass and a high-pass filter is that the low-pass signal still contains the influence of the more rapidly varying peaks. The *lower-envelope* technique (Schmahl & Kundu 1995) reduces this problem, and creates two signals which are much more independent. To obtain the lower envelopes, Schmahl and Kundu found the local minimum flux within a 155-day window scanned across the initial time series, and then smoothed the result with an 81-day boxcar. They then found the rotationally-modulated signal by subtracting the lower envelopes from the initial flux profiles. These rotationally- modulated curves then show the flux variability due to compact regions of spots and/or plage (Fig. 3). Note that, unlike the high-pass component, which would have zero mean, the rotationally-modulated component is always positive, with local minima close to zero.

2.1.   Thermal Bremsstrahlung or Gyro-resonance?

There has been some controversy about whether the microwave flux from active regions is due to thermal bremsstrahlung or gyro-resonance emission, which would then indicate whether the source of emission was the optically-thin corona or optically-thick sunspots. As early as 1958, Tanaka and Kakinuma showed that the spectrum of active regions had a spectral maximum around 5000 MHz, which indicated that gyro-resonance emission dominated. Later measurements over a wider frequency range confirmed this, and the observers (Tsuchiya & Takahashi 1968) concluded that active regions were 80-90% dominated by gyro-resonance emission.

More recently, however, Tapping and his colleagues (Tapping 1987; Tapping & Gaizauskas 1988; Tapping & DeTracey 1990) have argued that the 2800 MHz (10.7 cm) flux is produced mainly by free-free emission from coronal plasma, with a negligible fraction of gyro-resonance emission associated with sunspots. The coronal plasma overlies the plage, and so this assertion is equivalent to saying that the plage component of the microwave flux dominates the spot component.

One may assess these arguments by inspecting the 5-point spectra of the rotationally modulated and lower-envelope components using the Toyokawa fluxes (1000, 2000, 3750 and 9400 MHz) and the Ottawa 10.7-cm (2800 MHz) flux profiles. These are shown in Fig. 4. These 5-frequency spectra are all normalized to the same mean value, and are taken for times when there are a significant
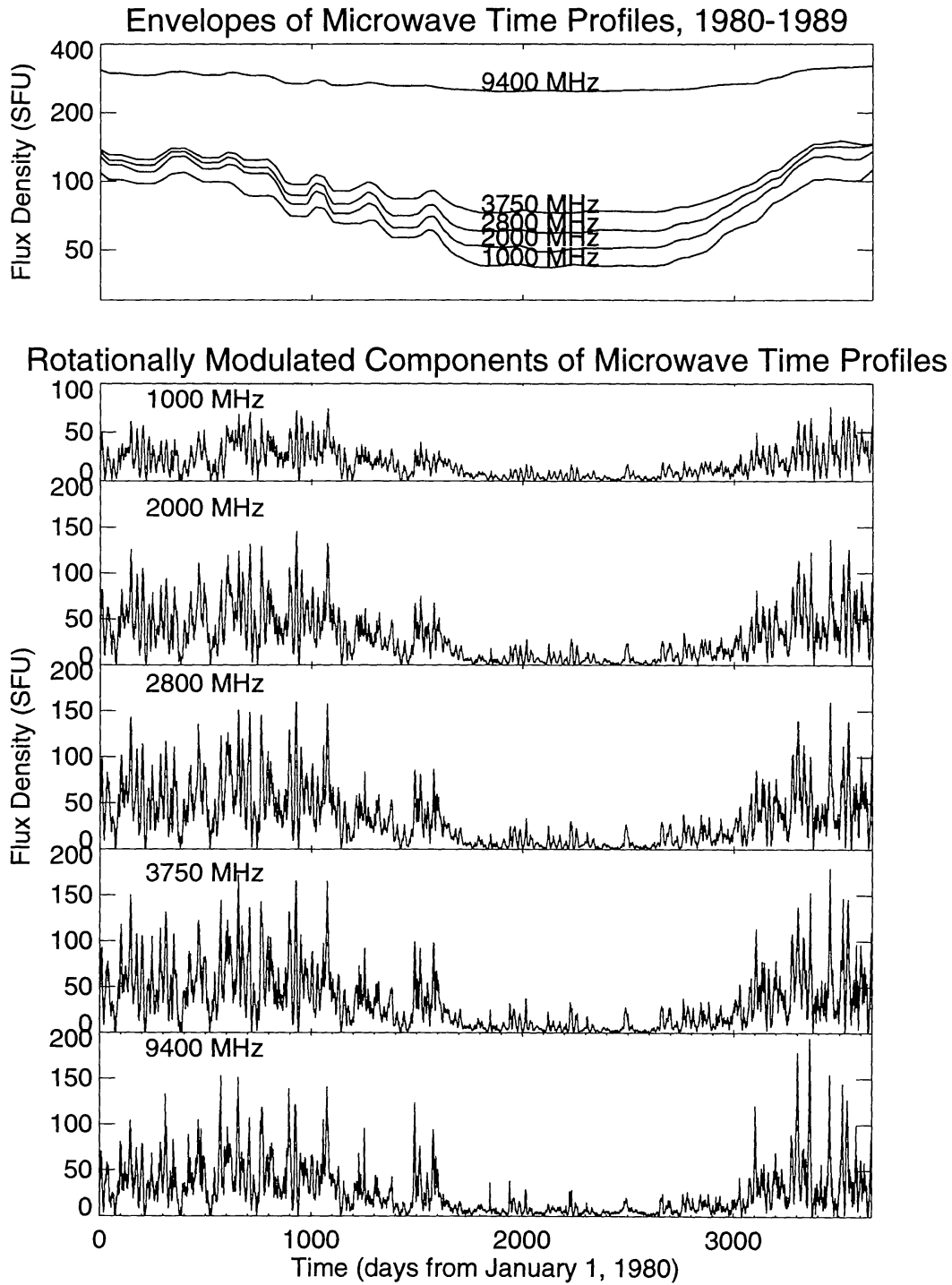
Figure 3.   Lower envelopes and rotationally-modulated profiles at the five microwave frequencies.
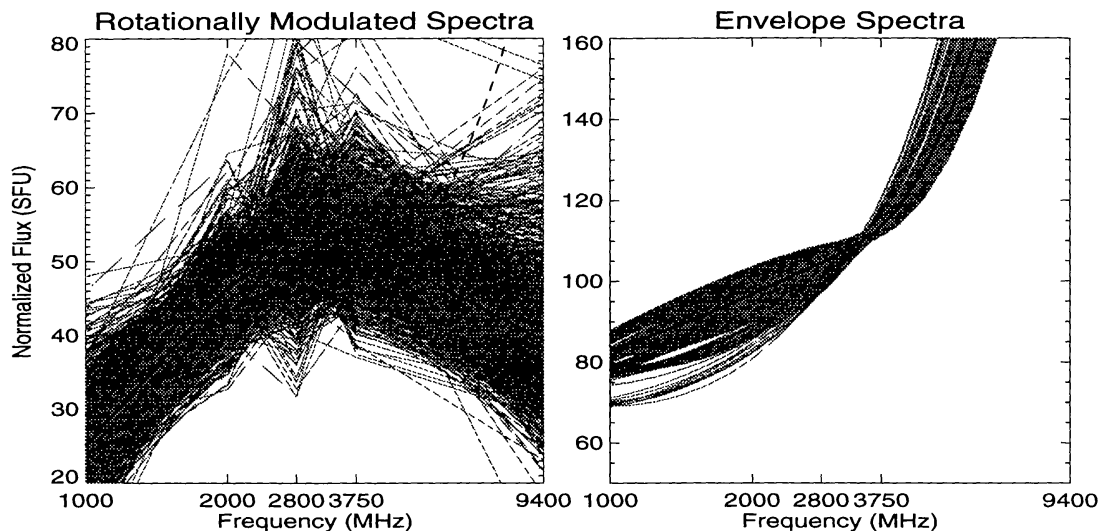
Figure 4.   The 5-point spectra of the rotationally-modulated (left) and lower-envelope (right) components using the Toyokawa fluxes (1000, 2000, 3750 and 9400 MHz) and the Ottawa 10.7-cm (2800 MHz) flux profiles.

number of spots on the Sun, that is, the Photometric Sunspot Index is high (PSI > 2.0). Note that the envelope spectra all steadily increase with frequency, the expected shape of a thermal bremsstrahlung spectrum. On the other hand, the rotationally-modulated spectra all have a maximum between 1000 and 9400 MHz. This is the shape expected for gyro-resonance emission spectra. This is evidence that sunspots are the major source contributing to the rotationally-modulated component of the total flux in the range $\sim 2000 - 8000$ MHz range. As Kundu (1965) pointed out, the spectral maximum could not be explained by free-free emission alone. "Piddington's theorem" (Piddington 1951) shows that, except at the low harmonics of the gyro-frequency, a free-free flux spectrum cannot have negative slope, or, equivalently, show a maximum.

2.2. Evidence from spatially-resolved spectra

However, one need not rely on the unresolved synoptic data to show this. Fig. 5 summarizes abundant evidence from spatially-resolved spectra in the cm-λ range that gyro-resonance emission (with peaked spectra) usually dominates the flux from active regions, while thermal bremsstrahlung emission (flat or rising spectra) comes from plage regions displaced from spots.

All of the observations summarized here support the contention that the peak of the flux spectrum (usually in the 3000-6000 MHz range) in the rotationally-modulated component is produced predominantly by gyro-resonance emission above sunspots. The fraction of spot-associated emission depends, of course, on the number and area of sunspots relative to the plage area, or more directly, on the projected area of coronal loops overlying the plage. The quoted observations also show that most of the 1000 MHz emission and the 9400 MHz emission is plage-associated. Because of this spectral dependence on the type of the source region it turns out to be possible, using regression analysis,
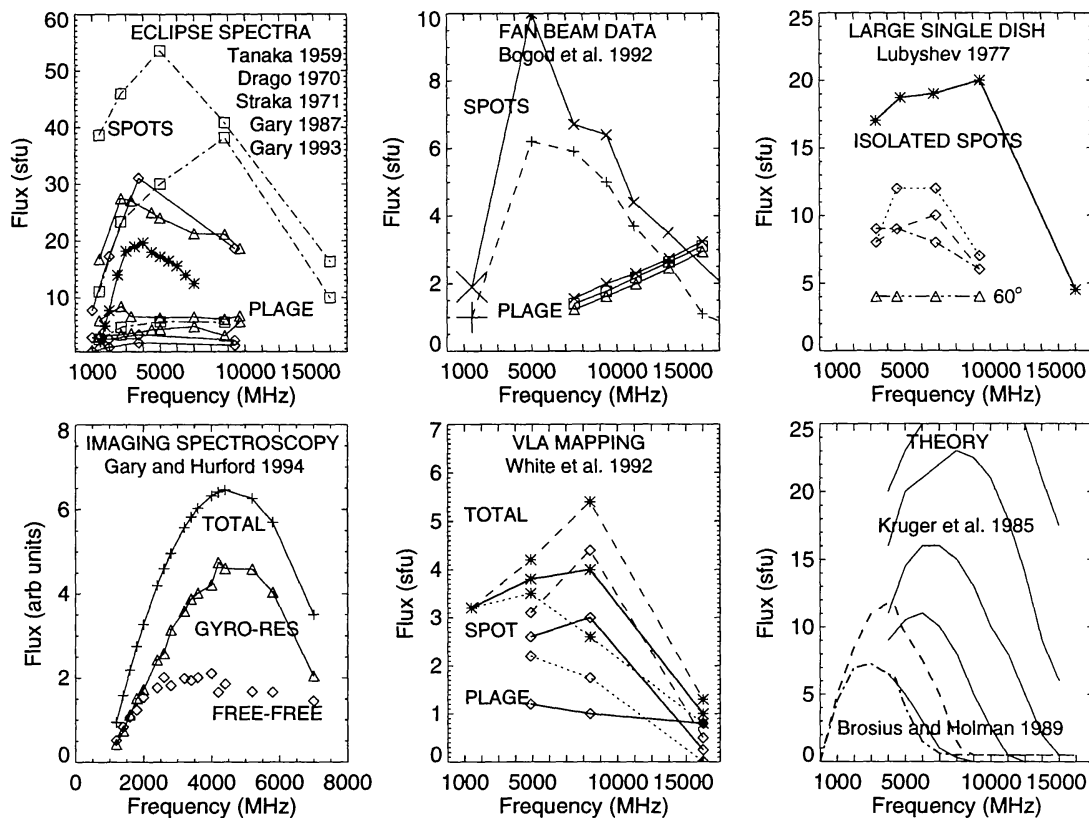
Figure 5. Evidence from spatially-resolved spectra in the cm-λ range that active regions are dominated by sunspot emission, and that the plage flux is relatively weak. (a) Eclipses, (b) Fan Beams, (c) Single-dish telescopes, (d) OVRO, (e) VLA, and (f) Theory.

to extract the fraction of sunspot-associated emission from the multi-frequency time series, and to generate good proxies for (a) sunspot area, (b) active plage area, and (c) quiet-sun chromospheric and coronal bremsstrahlung.

As the sunspot number varies through the solar cycle, we expect the contribution of the rotationally-modulated component to vary with time. Its fraction of the total flux is shown in Table 1 for yearly averages in the 1980–1989 period. In the most active years, the fraction at the intermediate frequencies is much larger than the fraction at 1000 and 9400 MHz. Thus the fraction spectrum is peaked much like the gyro-resonance spectrum, and this indicates that the free-free contribution is a smaller fraction of the modulated component in the active years. However, at solar minimum, the 1000 MHz fraction rises and becomes comparable to the 3750 MHz fraction. Hence the the spectrum of the rotationally-modulated component is flatter at solar minimum, indicating a larger contribution of plage-associated sources.

Table 1.   The percentage of the total flux that is rotationally modulated for the years 1980-1989.

ν	1980	1981	1982	1983	1984	1985	1986	1987	1988	1989
1000	18.3	21.1	29.1	21.3	19.8	10.4	9.5	14.5	18.9	23.2
2000	27.3	28.6	35.5	26.3	22.9	11.7	9.8	15.4	24.1	27.7
2800	28.8	29.9	35.8	25.0	21.9	10.1	8.5	14.1	23.9	26.0
3750	27.4	28.5	33.5	21.9	19.6	9.0	7.1	11.7	22.7	25.1
9400	11.2	12.5	14.4	7.0	6.5	2.6	2.4	3.3	8.1	11.4

3.   An Improved Proxy for Sunspots

It is possible to construct a spot proxy from single-frequency data using the envelope method. Based on the correlation coefficients determined by Schmahl & Kundu (1995), the best single-frequency spot proxies are 2800 and 3750 MHz. The poorest proxy is 1000 MHz, for which $r^2 = 0.60$, as compared with $r^2 = 0.80$ for 3750 MHz. Thus at the lowest frequency, not much more than half of the variance is spot-associated. The proxy is written in the form:

$$PSI = C_0 + \sum_{\nu} C_{\nu}^{rm} \times D_{\nu} + C_{\nu}^{env} \times E_{\nu}$$

where E_{ν} is the envelope signal, D_{ν} is the rotationally-modulated signal at frequency ν, the terms C_{ν}^{rm} are the five coefficients of the rotationally-modulated time series, and the C_{ν}^{env} are the five coefficients of the envelope time-series. The proxy has the best correlation with the PSI during the decay of cycle 21. During the time interval t=1435-2200 (days from January 1, 1980), the correlation is 93.4%. Overall, the RMS difference between PSI and spot proxy is 0.27 w/m^2, where the RMS value of PSI is 0.66 w/m^2. During the time interval spanning solar minimum through the rise of cycle 22 (t=1600-3020, or 4/84-3/88), the proxy has a better fit (though slightly lower correlation). The RMS difference between proxy and PSI is only 0.090 w/m^2 (13% of the RMS PSI). See Schmahl & Kundu (1995) for details.

Judging from the relative values in Table 2 and 1σ error bars of the coefficients in the regression, Schmahl and Kundu concluded that at all frequencies, both the rotationally-modulated and the envelope series are necessary for a good determination.

Table 2.   Proxy Coefficients for PSI

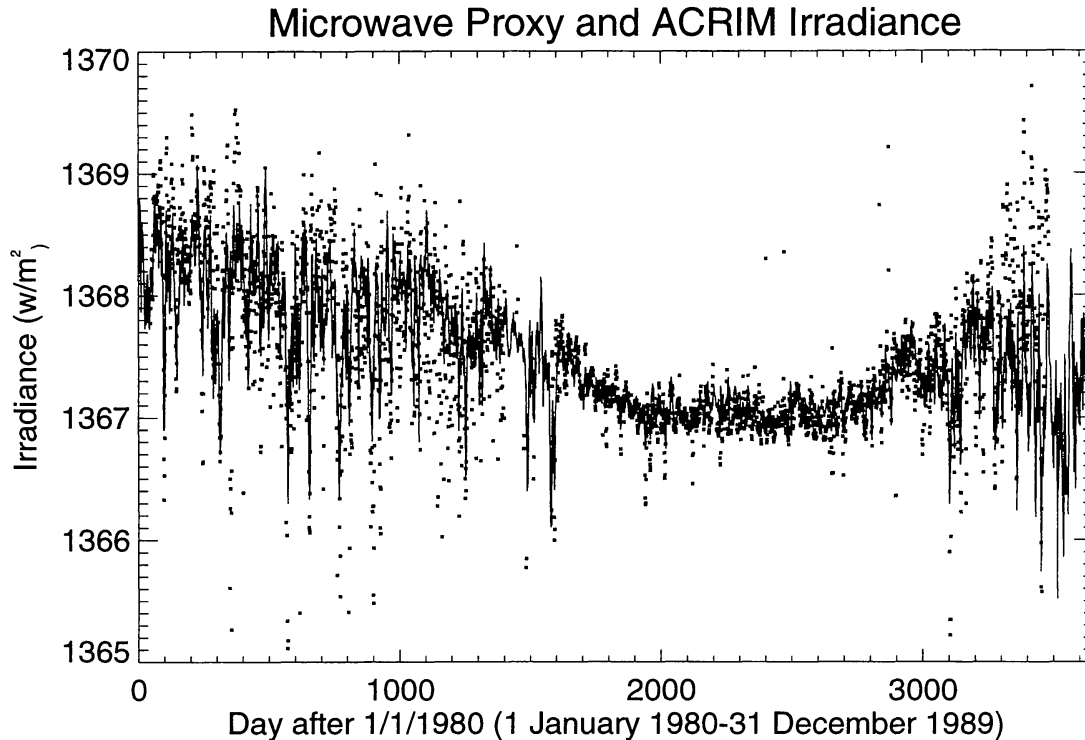| ν	C_{ν}^{rm}	σ_{rm}	C_{ν}^{env}	σ_{env}	t_{rm}	t_{env}
1000	0.003639	0.002108	-0.01635	0.008177	1.7262	-1.9996
2000	0.000851	0.006843	0.02567	0.006210	0.1243	4.1337
2800	0.008489	0.002225	0.00197	0.001318	-3.8147	1.4970
3750	0.025922	0.001583	0.00935	0.000980	-16.3798	9.5439
9400	0.030797	0.001245	0.00181	0.000703	24.7456	-2.5769

Figure 6.   Irradiance proxy (solid) overlaid on the ACRIM time series (dots).

4.   A Microwave Proxy for Irradiance

From the PSI proxy so determined, using linear regression again, Schmahl and Kundu obtained a microwave-based proxy for irradiance that is very close in quality to the proxy based on optical observations. Fig. 6 shows the proxy plotted for the decade of the 1980s along with the ACRIM irradiance. The RMS deviation between the microwave-based proxy and the ACRIM irradiance residuals for 1984-1990 (after the SMM repair) is 0.27 W/m^2, which is better than the deviation of 0.35 W/m^2 found using the microwave regression with ACRIM+PSI. This is about 10% of the peak-to-valley 1980-1989 irradiance range. Most of the discrepancies lie in rotationally-modulated variations, i.e. in the ACRIM "dips", but the longer-term variations are replicated quite well.

In the proxy for irradiance (Table 2), the rotationally-modulated coefficients are negative for 2000 and 3750 MHz. For 2000 MHz, the value of σ_{rm} is larger than C_ν^{rm} and Student's t-statistic is small, so the coefficient is not significantly different from zero. Similarly, the non-zero coefficient for 9400 MHz is not significant, as indicated by the small t-statistic in column 6). The reason for the negative coefficient at 3750 MHz is that (as mentioned in other contexts above), the rotationally-modulated microwave emission is mostly from sunspots, and the regression process automatically corrects for sunspot blocking. Student's t-statistics in this table also show that the coefficients with the highest significance are the rotationally-modulated and envelope components at 1000 MHz, and the rotationally-modulated component at 3750 MHz.

Table 3.   Proxy Coefficients for ACRIM Irradiance

ν	C_ν^{rm}	σ_{rm}	C_ν^{env}	σ_{env}	t_{rm}	t_{env}
1000	0.04214	0.00643	0.06388	0.00282	6.55074	22.67633
2000	-0.00114	0.00456	-0.07172	0.00633	-0.24890	-11.33599
2800	0.02921	0.00163	-0.00652	0.00212	17.95912	-3.07447
3750	-0.00469	0.00127	0.01477	0.00201	-3.70197	7.35457
9400	0.00014	0.00092	-0.02899	0.00149	0.15172	-19.46651

5.   Long-Range Stability of Microwave Measurements

For the post-SMM repair period, (1984-1989) when ACRIM was very stable, the RMS difference between the microwave proxy based on Toyokawa measurements and the irradiance signal is less than $0.2W/m^2$, out of a mean of $1368W/m^2$. Thus almost all of the short-term (days-weeks) irradiance variations are well-tracked. But even more interesting is that the long-range values were well tracked at this level. Assuming then, that the ACRIM instrument was stable to better than $0.1W/m^2$ (1 part in 10,000) per decade, in order to achieve comparable tracking by the proxy, the Toyokawa measurements must have had a very high calibration stability over that period. Fig. 8 shows a plot of the difference of the proxy and the irradiance over the life of SMM/ACRIM. The times when the spacecraft had poor pointing are excluded. The best-fit line to the difference time series shows a slight downward trend, amounting to $-0.3W/m^2$ in 10 years. This trend may not be statistically significant, but it is possible that it represents a long-term change in the calibration of the microwave measurements. The apparent drop of $0.3w/m^2$ translates into a flux change of 0.03 sfu, or on the average, 1 part in 3000 per decade.

This suggests that gaps of the order of a year in spacecraft irradiance data might be bridged by proxies. During a one-year period, the apparent stability of the Toyokawa measurements, combined with the current proxy, would provide an irradiance bridge with an uncertainty level significantly less than $0.1w/m^2$ over that interval.

6.   The Future of Synoptic Radio

6.1.   Extended use of existing data:

There is considerable room for extension of synoptic measurements to lower and higher frequencies (e.g. m, dm, mm), and we are beginning to see greatly expanded on-line availability of data (H. Coffey, this proceedings). We can look forward to the resumption of Toyokawa flux measurements (K. Shibasaki, this proceedings). As for the use of radio for proxies, with multi-frequency measurements there should be improved application to EUV and UV radiances. The gyro-resonance spectrum of the Sun can also provide a measure of the mean coronal magnetic field strength, giving a proxy of mean magnetic activity.

Many hundreds of days of solar radio observations by numerous workers have been obtained since 1977. It would be a labor of some effort, but also one of great value, to make maps from the existing archived visibility data using a
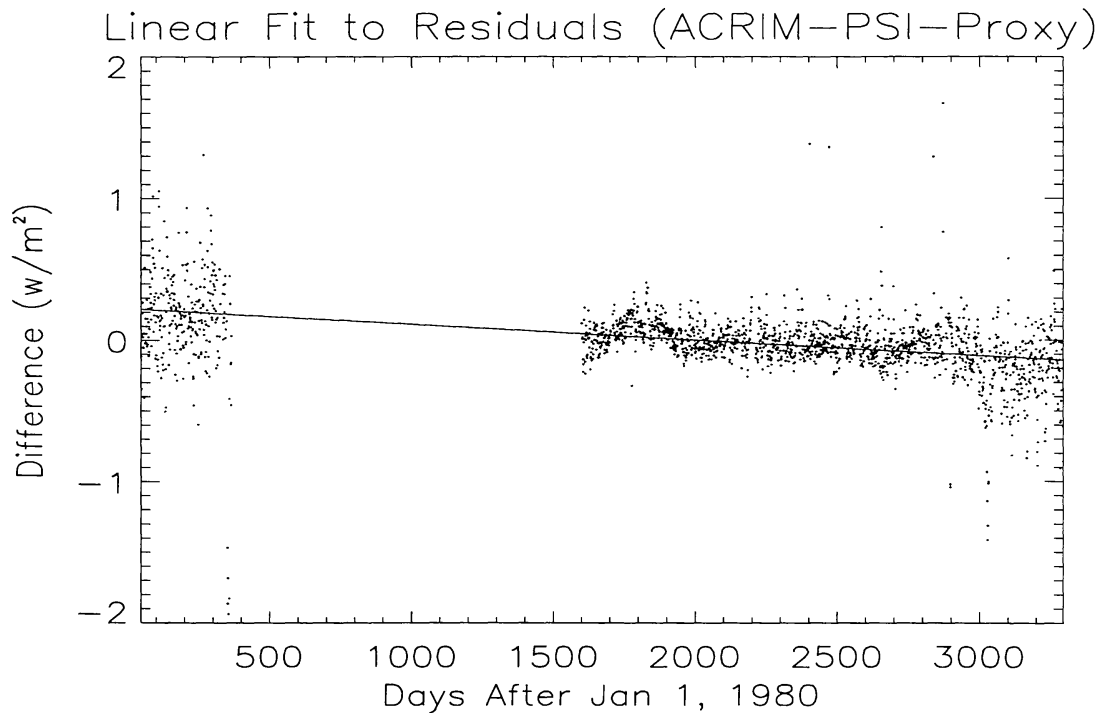
Figure 7. Plot of the difference between the proxy and the irradiance over the life of SMM/ACRIM.

standardized calibration. With automated techniques, this may become feasible in the near future. The automation of mapping and calibration proposed for Owens Valley points the way for simplified and standardized radio mapping on a daily basis.

6.2. Synoptic imaging with existing arrays

At the present time, synoptic cm-wave mapping of the Sun is performed at Nobeyama (17, 34 GHz), at the Siberian SRT (5.7 GHz), and at Owens Valley Radio Observatory (1-18 GHz). As Gary & Hurford (1994) have shown, multi-frequency imaging observations can provide "coronal magnetograms", coronal emission measures, and information about quasi-steady nonthermal sources.

6.3. Future telescopes

The proposed Frequency-Agile SRT (See T. Bastian, this Proceedings) may provide the best possible synoptic observations. This instrument will cover the frequency range 0.3-26 GHz (1-100 cm) with band spacing of $\Delta\nu/\nu = 0.05$. It will be able to map the full Sun, over 8-hour days, every day, with a spatial resolution of $\sim 1''$] and time resolution ~ 1 s.

There is also a possibility that millimeter-wave imaging can be done on a quasi-regular basis (at least during the summer months when sidereal observations are difficult) using the 11-antenna Berkeley-Illinois-Maryland Array.

For the purposes of long-range studies, one cannot over emphasize the importance (Tanaka et al. 1973) of having super-stable flux calibrations, so that

inter-comparisons of maps made years apart may be quantitatively compared, and that proxies of long-range changes of solar properties can be made with confidence in their reliability.

References

Bouwer, S. D. 1992, in Solar Electromagnetic Radiation Study for Solar Cycle 22, ed. R.F. Donnelly, NOAA ERL/SEL, p. 371

Covington, A. E. 1988, JRASC 82, 165-178

Denisse, J.F., 1948, Doctoral Thesis, University of Paris

Denisse, J. F., & Kundu, M. R. 1957, Comptes Rendus, 24, 45

Donnelly, Hudson, Pap, & Willson 1992, Solar Electromagnetic Radiation Study for Solar Cycle 22, (ed). R. F. Donnelly, NOAA ERL/SEL, p. 275

Gary, D., & Hurford, G. 1994, ApJ, 420, 903

Hinteregger et al. 1981, Geophys. Res. Lett., 8, 1147

Kundu, M. R., & Denisse, J. F. 1958, , Journ. Atmos. Terr. Phys., 13, 76

Kundu, M. R. 1965, Solar Radio Astronomy, New York, John Wiley and Sons

Neupert, W. 1992, Solar Electromagnetic Radiation Study for Solar Cycle 22, (ed. R.F. Donnelly), NOAA/REL/SEL, p. 360

Pap, J., & Tlamicha, A. 1992 Solar Electromagnetic Radiation Study for Solar Cycle 22, (ed). R.F. Donnelly, NOAA/REL/SEL, p. 76

Piddington, J. H. 1951, MNRAS 111, 45

Schmahl, E. J., & Kundu, M. R. 1994, Solar Phys. 152, 167

Schmahl, E. J., & Kundu, M. R. 1995, J. Geophys. Res. 100, A10, 19851

Tapping, K. F. 1987, J. Geophys. Res. 92, 829

Tapping, K. F., & Gaizauskas, V. 1988, JRASC 82, No. 5, 280

Tapping, K. F., & DeTracey, B., 1990, Chap. X, Sun in Time Conference, Tucson, AZ, Mar. 6-10, 1989 Solar Phys. (ISSN 0038-0938), 127, June 1990, p. 321-332

Tanaka, H., and Kakinuma, T., 1958, , Proc. Res. Inst. of Atmospherics, Nagoya Univ., 5, 81

Tanaka, H., Castelli, J.P., Covington, A.E., Krüger, A., Landecker, T.L., and Tlamicha, A. 1973, Solar. Phys., 29, 243

Tobiska, K.: 1992, Solar Electromagnetic Radiation Study for Solar Cycle 22, (ed. R.F. Donnelly), NOAA/REL/SEL, p. 338

Group Discussion

White: F10.7 from Ottawa/Penticton shows a very constant value of ∼68 sfu in all solar minima since 1947. Is this property also observed in the other records at different frequencies and observatories?

Schmahl: I have not yet looked at the digital data, since I only learned from Helen Coffey at this meeting that the data are all available over the internet. But now that they are available, I intend to have a look.

Coffey: We at NGDC put 55 stations' daily flux data, on-line on our web-site. These came from the IAUQBSA 1949-1986. You said that Tanaka headed an IAU Commission, who studied calibration methods and made recommendations to correct the datasets. Should NGDC make these corrections to the on-line data, or perhaps reference the Tanaka report?

Schmahl: I believe all the corrections had been put into the IAU Quarterly bulletins by about 1973, but it might be a good idea to reference Tanaka et al's paper (Solar Phys. 1973).

White: Radio observation offers estimates of coronal magnetic field strengths from strength of harmonics is gyroresonance emission. However, the results are controversial because field estimates have relatively high ($\sim$100G) relative to computed fields. Has this controversy been resolved by new experiments?

Schmahl: There is much better agreement now between models based on photospheric magnetograms and the radio-determined magnetic fields. The major uncertainty is the height of the gyro-resonance layer, but this can be determined by center-to-limb observations.

van Ballegooijen: Is the proposed Dedicated Solar Radio Telescope a single telescope or an array?

Schmahl: It would be an array of 20-30 small telescopes, like an expanded OVRO array or a small VLA.